Chem Soc Rev

Heterogeneous electron transfer at nanoscopic electrodes: importance of electronic structures and electric double layers

Journal:	*Chemical Society Reviews*
Manuscript ID:	CS-TRV-02-2014-000087.R2
Article Type:	Review Article
Date Submitted by the Author:	01-May-2014
Complete List of Authors:	Chen, Shengli; Wuhan University, Department of Chemistry Liu, Yuwen; Wuhan University, Chemistry Department Chen, Junxiang; Wuhan University, Department of Chemistry

Chem Soc Rev

RSCPublishing

REVIEW

Heterogeneous electron transfer at nanoscopic electrodes: importance of electronic structures and electric double layers

Cite this: DOI: 10.1039/xoxxoooooox

Received ooth January 2012,
Accepted ooth January 2012

DOI: 10.1039/xoxxoooooox

www.rsc.org/

Shengli Chen,* Yuwen Liu, and Junxiang Chen

Heterogeneous electron-transfer (ET) processes at solid electrodes play key roles in molecular electronics and electrochemical energy conversion and sensing. Electrode nanosization and/or nanostructurization are among the major current strategies for performance promotion in these fields. Besides, nano-sized/structured electrodes offer great opportunities to characterize electrochemical structures and processes with high spatial and temporal resolution. This review presents recent insights into the nanoscopic size and structure effects of electrode and electrode materials on heterogeneous ET kinetics, by emphasizing the importance of the electric double-layer (EDL) at electrode/electrolyte interface and the electronic structure of electrode materials. It is shown, by general conceptual analysis and recent example demonstrations of representative electrode systems including electrodes of nanometer sizes and gaps and of nanomaterials such as sp^2 hybridized nanocarbons and semiconductor quantum dots, how the heterogeneous ET kinetics, the electronic structures of electrodes, the EDL structures at electrode/electrolyte interface and the nanoscopic electrode sizes and structures may be related.

1. Introduction

Electron transfer (ET) is a fundamental process in physics, chemistry and biology. Heterogeneous ET at solid electrodes, a subject of theoretical and methodological foci in electrochemistry,[1,2] are of particular scientific and technological significance.[3,4] They on one hand are models for understanding various interfacial redox processes in chemistry and biology, and on the other hand are the basis of technologically relevant fields such as chemical and biological fuel cells, dye sensitive solar cells, sensors, molecular electronics, electrochemical synthesis, and so on. Recently, there have been growing fundamental and technological interests in using nanosized and nanostructured electrodes in electrochemistry.[4-7] They offer great opportunities to study electrochemical structures and processes with high spatial and temporal resolution. In the meantime, recent performance breakthroughs in various electrochemistry-based technologies have been largely relying on electrode nanosization and/or nanostructurization.[8-10] To unveil how the nanoscopic sizes and structures may impact the heterogeneous ET processes would provide guidance for material and electrode optimization in various electrochemical technologies and help to understand and control nanoscopic electrochemical characterization.[6] Besides, nanoscopic heterogeneous ET kinetics would also be of significance for the size and shape control in solution-based growth of nanomaterials which involves redox processes at solid/solution interfaces as the key steps.[11]

The nanoscopic sizes and structures of electrodes may affect heterogeneous ET kinetics in diverse ways. This review focuses on the enhanced effects of electronic structures of electrode materials and electric double-layer (EDL) structures at electrode/electrolyte interfaces due to the nanosization and/or nanostructurization. It is outlined as follows. First in Section 2, some fundamental elements of heterogeneous ET processes at electrode/electrolyte interfaces are presented, aiming at conceptually showing why in most cases the EDL and electronic structures take a minor part in the heterogeneous ET kinetics at conventional bulk metal electrodes and how they may become nontrivial in nanoscopic electrode systems. This section also provides an introduction to researchers from materials, nanoscience and other non-electrochemical fields working in electrochemical energy and sensing areas. Then in Sections 3-5, recent studies on the heterogeneous ET kinetics at electrodes of nanometer sizes and nanometer gaps and of nanomaterials including graphenes, carbon nanotubes (CNTs), and semiconductor nanoparticles are reviewed, by emphasizing the enhanced EDL and electronic structure effects related to nanosize and structures of electrodes and/or electrode materials. These representative nanoscopic electrode systems are of both fundamental and technological significance in electrochemistry and other related areas. Section 6 presents a brief discussion on

the possible EDL effects in ET processes relating to the quantum capacitance of nanomaterials. Section 7 summarizes the concluding remarks and outlooks.

2. Some fundamental elements of heterogeneous ET

2.1 Electrochemical interface and heterogeneous ET wherein

Upon bring an electrode into contact with electrolyte solutions, ET usually occurs between electrode and electroactive agents in solution till the electrode potential (E), which is a measure of the Fermi energy level (electrochemical potential) of electron in electrode, aligns with the equilibrium redox potential of solution species.[1,12] The ET processes would leave charges at electrode and in the meantime the accumulation and/or depletion of solution ions near the electrode due to electrostatic interaction, forming an EDL which is featured by gradient distributions of electrostatic potential and concentrations of ions. The EDL can be roughly divided into a compact and a diffuse part, with the boundary at the so-called outer Helmholtz plane (OHP), which is considered to the first approximation the place of the closet approach (PCA) of the solvated ions to the solvated electrode surface (Fig.1).[1,13] If there is no contact adsorption of ions at electrode surface, the potential should distribute itself linearly inside the OHP. The electrostatic potentials at electrode (φ_0) and at the OHP (φ_1) depend on E, the electronic structure of electrode and the dielectric property of solvent in EDL.[13] Eqn (1) gives the relation between φ_0 and E, where μ_e is the chemical potential of electron in electrode, which represents the non-electrostatic part of the electronic work function of electrode and can be manifested by the shift of the Fermi level from the bottom of the electron energy band of electrode.

$$E = -\mu_e / F + \varphi_0 \quad (1)$$

For ordinary bulk metal electrodes which have high density of states (DOS) near Fermi levels, ET hardly modifies μ_e, therefore result in considerable change in the charge density at electrodes and therefore φ_0. To this end, the change in the electrode potential (ΔE) approximately equals the change of electrostatic potentials at electrode ($\Delta\varphi_0$), regardless of electrode materials. In electrochemistry, the electrode potentials are usually quoted with respect to a reference point,[1] for example, the standard equilibrium electrode potential (E^0). Since that $E\text{-}E^0 \approx \varphi_0\text{-}\varphi_0^0$, the electrode potential is mostly not distinguished with the electrostatic potential for metal electrodes in conventional electrochemistry. However, one has to bear in mind that $E \neq \varphi_0$. At certain E, the φ_0 and the charge density at electrode surface and therefore the EDL structure would differ for different electrode materials. In most cases this matters little in interfacial ET kinetics since the latter is negligibly affected by the EDL structures at conventional bulk metal electrodes. In the cases when the EDL effect is significant in the heterogeneous ET kinetics, the electrode materials could become important. In a recent study, Mirkin and co-workers observed different apparent rate constants for hexaammineruthenium(III) ($Ru(NH_3)_6^{3+}$) reduction on nanometer sized Pt and Au electrodes,[14] while previous studies at bulk electrodes of different materials gave similar rate constants for this redox probe.[15,16] This may be a result of the increased EDL effect in the heterogeneous ET processes at nanometer-sized electrodes.[5,6,17-21]

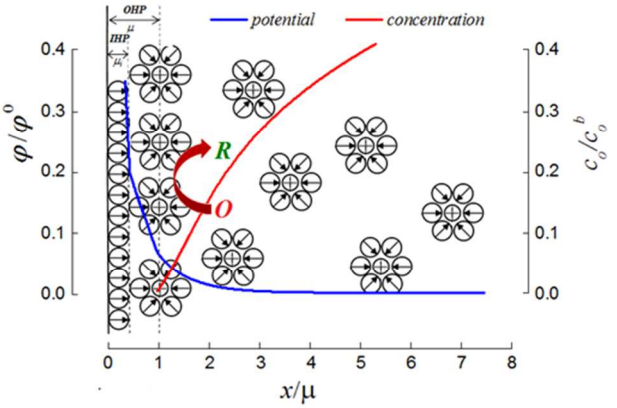

Fig. 1 A schematic diagram of the structure of an electrode/electrolyte interface. The blue and red solid lines illustrate the distributions of the electrostatic potential and the concentration of reactant respectively.

An heterogeneous ET process can proceed continuously upon electron injection/extraction into/from the electrode by using an external bias. When the ET rate (v_{et}) equals to the rate of electron injection/extraction, there will be no change in the charge density (therefore φ_0) and μ_e at the electrode. Accordingly, E stays constant. In this case, $j=nFv_{et}$, where j is the current density at electrode surface and n is the electron number in the ET reaction. If $j>nFv_{et}$, the electron injection/extraction would result in changes in E, the charge density at electrode and the EDL structure at interface, which in turn increase v_{et} till j and v_{et} are balanced.[1]

In the course of a continuous ET process, there would form a concentration distribution layer (CDL) of electroactive species in the solution due to the finite mass transport rate,[1] which approximately starts at the OHP and spans a considerable region into the solution (Fig. 1). The mass transport of electroactive species in CDL determines their concentrations at the OHP, which are related to v_{et} according to

$$v_{et} = k_c c_O^{OHP} - k_a c_R^{OHP} \quad (2)$$

where k_c and k_a refer to the rate constants of the reduction and oxidation directions at the applied electrode potential, c_O^{OHP} and c_R^{OHP} are the concentrations of the oxidized and reduced agents at the OHP where the ET is assumed to take place.

Since the CDL and the diffuse EDL start similarly at the OHP, one can imagine that they should merge into each other during an ET process. For the sake of simplicity, however, the overlap between the EDL and CDL has been generally ignored in conventional electrochemistry, due to that under usual electrochemical conditions the EDLs, which are from a few angstroms to tens of nanometers in thickness depending on the concentrations of electrolyte ions, are negligibly thin as compared with the CDL (typically several to hundreds of micrometers in thickness).[1] Thus, the concentration distributions of redox species are negligibly affected by the electrostatic potential distribution in the EDLs, and in the meantime the electrostatic potential distributions in the EDLs are little affected by the mass transport of redox species. Accordingly, the CDL and EDL can be treated separately, with the former assumed to be in electroneutrality and the latter

treated with the equilibrium Poisson-Boltzmann theories even when ET reactions occurs, for example, as did in the well-known Frumkin treatment of the diffuse EDL effects.[1] As will be shown in Section 3, this may become problematic in nanocopic electrode systems, where the CDL becomes comparably thin with the diffuse EDL.[17-21]

2.2 Heterogeneous ET kinetics based on transition-state-theory

The earlier versions of the heterogeneous ET theories have been constructed by adopting the concepts in homogeneous chemical reaction kinetics, central to which is the idea that reactions proceed through a well-defined transition state (TS) located at the crossing of the free energy curves of the reactant and product systems (RS and PS). To translate this treatment to heterogeneous ET reactions, one simply includes the electron in the RS or TS (Fig. 2).[1] Since that E is related to the molar free energy (the electrochemical potential) of electron at electrode, the free energy curve of the RS or PS thus would be modulated by E.

For a one-electron outer-sphere heterogeneous ET reaction, $O+e^- \leftrightarrow R$, the free energy curves of RS and PS are respectively,

$$G_{O+e^-}(q) = \Delta G^0 + zF\varphi_1 + f_O(q) - FE \quad (3)$$

$$G_R(q) = f_R(q) + (z-1)F\varphi_1 \quad (4)$$

in which ΔG^0 is the so-called standard free energy of reaction referring to the molar free energy difference between the PS and RS at their equilibrium configurations (Fig. 2), z is the charge of O, and q refers to the nuclear configuration coordinates. The functions of $f_O(q)$ and $f_R(q)$ describe the corresponding free energy curves, which are zero at the equilibrium configurations. The terms containing φ_1 correspond to the free energies required to bring a mole of O or R to the OHP. ΔG^0 represents the thermodynamic driving force for an ET process, which can be expressed as

$$\Delta G^0 = F(E-\varphi_1) - F(E^0-\varphi_1{}^0) \quad (5)$$

in which $\varphi_1{}^0$ is the electrostatic potential at the OHP as $E=E^0$. Under usual electrochemical conditions (e.g., at bulk metal electrodes and in the presence of excess of supporting electrolyte), φ_1 (or $\varphi_1{}^0$) is negligibly small as compared with E (or E^0). Therefore, Eqn (5) becomes the usual expression of ΔG^0 commonly seen in electrochemical literatures, that is,

$$\Delta G^0 \approx F(E-E^0) \approx F(\varphi_0-\varphi_0{}^0) \quad (6)$$

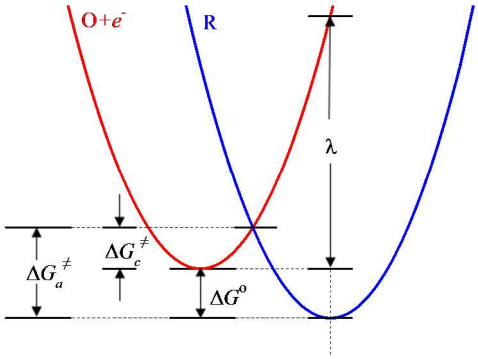

Fig. 2 Crossing of free energy curves of RS and PS for a one-electron outer-sphere heterogeneous ET reaction, $O+e^- \leftrightarrow R$.

By changing E, the free energy curve of ($O+e^-$) will be shifted upward or downward, resulting in changes in the crossing point and ΔG^0. Accordingly, the activation free energies for the reduction and the oxidation direction ($\Delta G_c^{\neq}$ and $\Delta G_a^{\neq}$) are modulated. The ways of $\Delta G_c^{\neq}$ and $\Delta G_a^{\neq}$ varying with E depend on the formalisms of $f_O(q)$ and $f_R(q)$ used, which have led to different heterogeneous ET kinetic models, for examples, the Butler-Volmer (BV) and the Marcus theory respectively.[1]

The BV model has been the most extensively used formalism for electrochemical kinetics since its inception in the early 1930s due to Butler and Volmer.[1] It assumes that the change in the driving force (ΔG^0) is split into two fractions: one in favour of the rate of reduction or oxidation (α), and the other in disfavour of the rate of oxidation or reduction (1-α). The so-called transfer coefficient (or symmetry factor), α, is considered independent of E. Thus, $\Delta G_c^{\neq}$ and $\Delta G_a^{\neq}$ would change linearly with E. This is similar to the Brønsted-Evans-Polanyi (BEP) (also called linear free energy) relation in heterogeneous catalysis, which correlates the free energy of activation with the free energy of reaction in a linear form without considering the details about the activation process. The linear free energy relation implies that the free energy curves can be considered linear at their cross point. Considering that any curves can be reasonably linearized in a narrow region around a point by performing the Taylor series expansion, one can imagine that the BV theory should apply only at potentials very close to E^0.

The Marcus theory, which will be denoted as classic Marcus-Hush (MH) theory in the following, was originally developed by Marcus for homogeneous ET kinetics in solutions and was adopted to treat heterogeneous ET kinetics mainly by Marcus and Hush.[2,22] In comparison with the phenomenological BV theory, the MH model provides physical insight into the activation of an ET process, namely, the reorganization of the inner ligands in the redox species together with the outer solvent shells of redox species to reach the iso-energetic electronic states at which electron tunneling occurs according to the Frank-Condon principle.[1,2] By assuming that the reorganization involves only harmonic fluctuations of nuclear configuration coordinates of redox species and the position and orientation of the solvent molecules, and that $f_O(q)$ and $f_R(q)$ have the same quadratic form, the activation free energies for the reduction and the oxidation directions are given as

$$\Delta G_{c/a}^{\neq} = \frac{\lambda}{4}\left(1 \pm \Delta G^0/\lambda\right)^2 \quad (7)$$

in which λ is the so-called reorganization energy (Fig. 2). The $\pm$ take plus and minus for reduction and oxidation respectively. According to Eqn (7), one obtains

$$\frac{\partial \Delta G_{c/a}^{\neq}}{\partial \Delta G^0} = \frac{1}{2}\left(1 \pm \Delta G^0/\lambda\right) \quad (8)$$

which predicts a linear relation between $\Delta G_{c/a}^{\neq}$ and ΔG^0 as $\Delta G^0 << \lambda$. This should be satisfied as E is close to E^0 or λ is very large. To this end, the BV model is just a simplified version of the MH model for heterogeneous ET kinetics at electrode potentials close to E^0 and or for ET reactions with very large λ, although the BV theory was developed much earlier. Eqn (8) also predicts a symmetric transfer coefficient of 0.5 for the reduction and oxidation directions. This is due to that the same symmetric parabolic function has been assigned to $f_O(q)$ and $f_R(q)$. Actually, most of the outer-sphere heterogeneous ET reactions exhibit α values near 0.5. There are examples

showing the weakness of the symmetric MH model. The interested readers may refer to recent review by Compton and co-workers.[23]

Based on the transition-state-theory, the rate constants for the oxidation/reduction (a/c) directions of an ET process satisfy

$$k_{a/c} = k^0 \exp\left(\pm F(E-E^0)/2RT\right)\exp\left(F^2(E-E^0)^2/4\lambda RT\right) \quad (9)$$

where $k^0=v_n k_{el}\exp(-\lambda/4RT)$, is the so-called standard rate constant, which refers to the equalized rate constants for reduction and oxidation directions at $E=E^0$ where $\Delta G^0=0$ and $\Delta G^{\neq}=\lambda/4$. As $E-E^0<<(\lambda RT)^{1/2}/F$, Eqn (9) reduces to the rate constant expressions in the BV theory with a transfer coefficient of 0.5, although in the BV theory no explicit expression has been given for k^0. Please note that E and E^0 should be replaced respectively by $E-\varphi_1$ and $E^0-\varphi_1^0$ when considering the possible EDL effects.

In above k^0 expression, v_n ($\approx k_b T/h$) is the effective nuclear frequency to take the RS to the crossing point, and k_{el} is the electronic transmission coefficient representing the electron transition probability at the crossing point, which is given as Eqn (10) according to the Landau-Zener model[24],

$$k_{el} = 2(1-\exp(-v_{el}/2v_n))/(2-\exp(-v_{el}/2v_n)) \quad (10)$$

where $v_{el}=2h\pi^{3/2}H^2(\lambda k_b T)^{-1/2}$ is the electron hopping frequency at the crossing point, H is electronic coupling matrix element between electrode and redox agent, and k_b and h are the Boltzmann and Planck constants respectively. Depending on H, which has an energy unit characterizing the electronic interaction strength between electrode and redox agent, the value of k_{el} lies between zero and one. For small H corresponding to weak interaction, Eqn (10) predicts a continuous increase of k_{el} (therefore ET rate constant) with H. This type of ET processes are considered non-adiabatic. As H reaches some large values, k_{el} approaches a constant value of 1 according to Eqn (10). The ET processes then proceeds in adiabatic mode. The adiabaticity of an heterogeneous ET process and its relation with the electronic structure of electrode will be discussed in the following.

2.3 Electronic structure views of electrochemical ET kinetics

In the classic BV and Marcus–Hush models, the electrode potential is considered to affect ET rate by changing ΔG^0 with FE. In doing so, it has been assumed that the electrons involved in a heterogeneous ET processes all have the same free energy as those at the Fermi level of electrode, or in another word, that only the electron states near the Fermi level of electrode participate ET process. Therefore, all the redox molecules have to be brought to the same activation transition state possessing a frontier electronic state (HOMO for O, and LUMO for R) aligned with the Fermi level of electrode. This is obviously unrealistic when considering that solid electrodes generally have a continuum of energy band with considerable width and that the frontier electronic states in the redox molecules may fluctuate over a range of energy due to various structural relaxation (Fig. 3). In reality, any occupied electronic state in an electrode is eligible for reductive ET as far as its energy level falls into the fluctuation range of the LUMO of O; likewise, any unoccupied state in an electrode with energy level within the fluctuation range of the HOMO of R can accept electrons. In the other words, all possible configurations of the redox agents may serve as the activation transition states in a heterogeneous ET, rather than only those having frontier electronic state aligned with the Fermi level of electrode. The classic MH and BV formalisms have simplified the multi-level, multi-state heterogeneous ET into an equivalent narrow one-level, two-state ET around the Fermi level, which should be reasonable only as E is not far away from E^0.

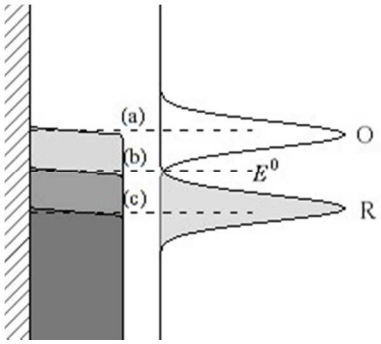

Fig. 3 Schematic illustration of multi-level, multi-state nature of heterogeneous ET at electrochemical interface between a metal electrode and redox couple O/R. Filled states are denoted by the gray shading. Electrode states are given for three representative electrode potentials: (a) $E>E^0$, (b) $E=E^0$ and (c) $E<E^0$.

The concept of the multi-level and multi-state nature of the heterogeneous ET processes at electrode/electrolyte interfaces has rooted to the earlier works of Levich[25] and Gerischer[26]. One of the main implications of these works is that the heterogeneous ET rates would be proportional to the electronic overlap integral between the metal surface and the redox agent and to the electronic DOS near the Fermi level of the electrode.[25] However, experimental measurements using electrodes of different metals[15] and metals modified with different ad-atoms deposited at underpotential[16] have shown little difference in the rate constants for certain redox couples, even when the DOS near the Fermi level differs by an order of magnitude. This has been interpreted in terms of the adiabatic nature of heterogeneous ETs at bare conducting electrodes.[27] Only when an ET process proceeds in non-adiabatic mode, that is, under weak electronic interaction between electrode and redox agents, ET rate may exhibit electronic structure dependence. ET at electrodes covered by thin insulating films are believed to proceed non-adiabatically.[28-30] There are two major types of theoretical models in the literatures to account for the adiabaticity transition of the multi-state heterogeneous ET, in both of which the structural relaxation of redox agents is treated classically with the harmonic fluctuation as that in the MH model, while the electron exchange between electrode and redox agents is modeled in the level of quantum mechanics.

Schmickler et al[27] adopted the Anderson-Newns model Hamiltonian to treat the heterogeneous ET. In this model, the electronic coupling between electrode and redox agent was described with a small energy level broaden of the frontier orbital in redox molecule (Δ), which depends on the electronic coupling matrix element and electrode DOS according to its definition. The model produced equations relating the energy and electron occupation probability of redox molecule with Δ. These equations predicted a potential energy curve exhibiting two minima, which correspond to the reduced and the oxidized

states respectively, separated by a barrier of height close to $\lambda/4$ at relatively small Δ ($<<\lambda$), thus seemingly to imply the independence of ET rate on the electronic coupling under weak adiabatic condition. However, the model also predicted a continuous lowering of energy barrier with increasing the Δ at relatively large Δ, thus seemingly to suggest that there is a relatively strong adiabatic region where heterogeneous ET rates depend on electrode nature. It seems that there has hitherto been no evidence to support the existence of such adiabatic ET systems. Since the electronic transitions between electrode and redox agent at different energy levels of electrode continuum are considered as a whole, this model is actually somewhat a quasi-two state model. Indeed, it recovers the classic MH behaviors under relatively small Δ. This model seems also exhibiting some weakness in predicting the ET rates at potentials significantly departing from E^0.

Another multi-state heterogeneous ET model which accounts for the adiabaticity transition is based on quantum perturbation method. The earliest version of this model was developed by Dogonadze et al.[31] In this model, the electron exchanges at different electronic states of electrode continuum are treated independently. Thus, an heterogeneous ET reaction can be considered to occur via a manifold of reaction surfaces, each corresponding to a different electronic orbital on electrode. It was argued that even though the transition probability for each surface might be small, the total transition probability can still be unity if a sufficient number of such surfaces are available. By assuming classical harmonic mode of structural fluctuation of redox agents, the ET rate constant at a certain electronic energy level of $-F\varepsilon$ (ε here has the unit of potential) can be described with the MH formalism by substituting ε for E in Eqn (9). The overall rate constants for the oxidation/reduction (a/c) are

$$k_{\mathrm{a/c}} = \int_{-\infty}^{+\infty} v_n k_{\mathrm{el}}{}^{\mathrm{a/c}} A^{-1} \exp(-(F(\varepsilon - E^0) + \lambda)^2 / 4\lambda RT)\mathrm{d}\varepsilon \quad (11)$$

where $A=(4\pi\lambda RT)^{1/2}$ is a normalization factor ensuring the total configuration probability of a redox agent to be 1. The terms of $A^{-1}\exp(-(F(\varepsilon-E^0)+\lambda)^2/4\lambda RT)$ and $A^{-1}\exp(-(F(\varepsilon-E^0)-\lambda)^2/4\lambda RT)$ are respectively the probability densities of O and R to have the configuration with a frontier electronic state of $-F\varepsilon$ energy. Although the integral limits cover all energy levels, the integrand has a significant value only when there is visible overlap between the donating and receiving electronic states. The overlapped areas vary with the electrode potential E. In Fig. 3, the oxidation is blocked in the case (a) since that the filled R states overlap little with the unoccupied electrode states, while in the case (c) the reduction is blocked since the empty O states overlap little with the occupied electrode states.

For multi-state ET at each energy level, the total electron hopping frequency for the reduction and oxidation directions should be $v_c=\rho_\varepsilon f(\varepsilon)v_{\mathrm{el}}$ and $v_a=\rho_\varepsilon(1-f(\varepsilon))v_{\mathrm{el}}$, in which ρ_ε is the DOS at the energy level of $-F\varepsilon$ in the electrode, and $f(\varepsilon)=(1+\exp(F(\varepsilon-E)/RT))^{-1}$ is the *Fermi function* referring to the corresponding electron filling probability. The electronic transmission coefficient for each energy level thus can be obtained according to Eqn (10) by substituting v_c or v_a for v_{el}, that is,

$$k_{\mathrm{el}}{}^{\mathrm{a/c}} = 2(1-\exp(-v_{\mathrm{a/c}} / 2v_{\mathrm{n}})) / (2-\exp(-v_{\mathrm{a/c}} / 2v_{\mathrm{n}})) \quad (12)$$

Thus, $k_{\mathrm{el}}{}^{\mathrm{a/c}}$ depends on the product of $H\rho_\varepsilon$. Even if H is some small, k_{el} could be 1 when ρ_ε is very large, which is true for usual bulk metal electrodes. Therefore, ET processes at bare metal electrodes would be approximately independent on the nature of electrode. In the cases when H is very small, for example, when ET takes place at electrode covered by thin insulating films, $k_{el}{}^{\mathrm{a/c}}$ may be less than 1 and vary with H and ρ_ε. This non-adiabatic nature could make the ET rates sensitive to electrode materials.

According to Eqn (12), $k_{\mathrm{el}}{}^{\mathrm{a/c}}$ can be approximately simplified into $v_{\mathrm{a/c}}/v_{\mathrm{n}}$ when $v_{\mathrm{a/c}}$ are very small. Thus, the rate constants for nonadiabatic ETs can be expressed by Eqn (13), which is equivalent to that given by Levich et al[25] and by Chidsey[28] and tells that the heterogeneous ET rates are proportional to H and ρ_ε.

$$k_{\mathrm{a/c}} = \int_{-\infty}^{+\infty} v_{\mathrm{a/c}} A^{-1} \exp(-(F(\varepsilon - E^0) + \lambda)^2 / 4\lambda RT)\mathrm{d}\varepsilon \quad (13)$$

Considering that in most of metal materials ρ_ε is nearly invariant in a wide range of energy levels around Fermi level, it can be replaced by the DOS around the Fermi level, ρ_f. If we further assume that H is also independent on ε, the rate constants for both the non-adiabatic and adiabatic ETs can be unified in the following general form,[32]

$$k_{\mathrm{a/c}} = k^{\mathrm{BV}}{}_{\mathrm{a/c}} \frac{\int_{-\infty}^{+\infty} \frac{\exp(-F^2(\varepsilon - E^0)^2 / 4\lambda RT)}{2\cosh(F(\varepsilon - E)/2RT)} d\varepsilon}{\int_{-\infty}^{+\infty} \frac{\exp(-F^2(\varepsilon - E)^2 / 4\lambda RT)}{2\cosh(F(\varepsilon - E)/2RT)} d\varepsilon} \quad (14)$$

in which $k^{\mathrm{BV}}{}_{\mathrm{a/c}}=k^0\exp(\pm F(E-E^0)/2RT)$ refers to the rate constant expressions given in the BV theory. In the non-adiabatic case, k^0 depends on H and ρ_f, while it doesn't for the adiabatic ETs.

According to the model by Dogonadze et al, one would expected that k^0 varies with ρ_f even on bare electrodes of materials with very low DOS near the Fermi level. The much slower ET rates for outer-sphere redox systems on silicon and other semiconductor surfaces at potentials within the band gap may be a prominent example of non-adiabatic heterogeneous ET due to low electrode DOS. This and related phenomena are the basis of the large body of research on semiconductor electrochemistry.[1,12] Recent electrochemical mapping studies using scanning electrochemical microscopy (SECM) and scanning electrochemical cell microscopy (SECCM) by Unwin and coworkers[33] have also demonstrated direct correlation between heterogeneous ET kinetics and the local DOS on the surface of polycrystalline boron-doped diamond (pBDD), which is a well-known heterogeneous electrode material and has semiconductor or quasi-metal electronic properties depending on boron doping level. As will be reviewed later on in Section 4 and 5, low DOS resulted non-adiabatic heterogeneous ET also occurs on electrodes of nanomaterials such as graphenes, CNTs and semiconductor nanocrystallites.

For the sake of convenience, we will denote the heterogeneous ET kinetic model described by Eqn (14) as "DOS-based model" in the following. According to this model, the rate of a heterogeneous ET reaction would reach a limiting value as E significantly departs from E^0, rather than undergoes an inversion as predicted by the MH formalism or increases unlimitedly as predicted by the BV formalism. The deviation of the classic MH and BV prediction from that of Eqn (14)

depends on the reorganization energy of the redox agents.[28, 32, 34-36] Larger the λ is, less deviation of the BV and MH prediction can be seen. This is due to that larger λ corresponds to sharper DOS distribution of redox molecule, which makes the contribution of the non-Fermi states in electrode insignificant to the overall ET rate. For typical λ around 100 KJ/mol, the MH formalism predicts very similar potential dependence of rate constants with Eqn (14) prior to the occurrence of the Marcus inversion, while the BV prediction exhibits deviation as $|E–E^{0\prime}|$ is larger than 0.2V.[34] In conventional macroscopic electrode systems, electrode processes usually reach the limiting mass transport control at moderate overpotentials, where the ET kinetics insignificantly deviate from the prediction of the BV and MH models.

3. Heterogeneous ETs at nanosize and nanogap electrodes

Nanosize and nanogap electrodes have received considerable recent interests in electrochemical fundamental studies and sensing application. The former, which are also known as nanoelectrodes including nanosphere, nanocone, nanodisk, nanoband and nanowire electrodes, possess nanoscale exposed electroactive sizes at least in one dimension.[5,6] The latter refer to two biased electrodes located in close proximity to each other, which allow repetitive oxidization and reduction of dissolved redox molecules. Nanofludic thin-layer cells represent a typical nanogap electrode system.[8,36] SECM, in which a nanoelectrode tip is placed in close proximity to a substrate electrode surface, involve both nanosize and nanogap electrodes.[1,37] These electrode systems share a number of common features. They offer extremely high mass transport rates of electroactive species toward/from working electrodes, therefore have been among the major current approaches to investigate the kinetics of fast heterogeneous ET reactions which are inaccessible to conventional large electrode systems.[14,37-39] In addition, they are commonly used in studying the electrochemistry of single molecules, nanoparticles, biological cells and enzymatic catalysts due to the extremely small sizes and/or confined spaces.[5-8] More importantly, they could be model systems for understanding some nanoscopic features of heterogeneous ET kinetics widely involved in wet chemical fabrication of nanomaterials, solution-based SPM characterization, and so on.

There are two typical nanoscopic ET kinetic features in these electrode systems, both of which are related to the greatly enhanced mass transport rates. First, the high mass transport rates would push the ET kinetics governed voltammetric responses to potentials where the phenomenological BV model and even the more physical MH model become inappropriate.[34, 40] Besides, the significant reduction of CDL thickness, which is the origin of the high mass transport rates, would raise pronounced EDL effects on the kinetics of heterogeneous ETs.[17,19-21,40]

3.1 On the failure of the linear free energy relation and the quasi-two state ET assumption

Although the multi-state nature of heterogeneous ET has been recognized since early 1970s,[25,26] it was brought to attention substantially in early 1990s when the inapplicability of the quasi-two state BV and MH models was demonstrated in the framework of non-adiabatic ETs between electrodes and electroactive agents spaced by a self-assembled monolayer (SAM).[28-30] By attaching the redox agents on the end of a SAM, the heterogeneous ET kinetics can be investigated in a wide range of potentials without the mass transport limitation. For electrode processes involving free moving redox agents, the BV model has remained the major theoretical approach for kinetic analysis.[1] In the last a few years, however, the weakness of the BV and even the classic MH formalism in treating the heterogeneous ET kinetics revived considerable attention when the voltammetric responses of nanoscopic electrode systems are concerned.[32, 34-37]

To overcome the inappropriateness of the linear free energy relation incorporated in BV model in relatively large range of potentials, Liu et al have used the classic MH model to treat the ET kinetics at nanodisk electrodes.[40] Later Feldberg[32] compared the voltammetric responses of nanodisk electrodes predicted by the BV and DOS-based models in terms of the reversibility of an electrode process, which can be evaluated according to $\gamma=k^0r_0/D$ (r_0: electrode radius; D: diffusion coefficient of the redox species), and the reorganization energy λ. It was concluded that significantly different voltammetric responses will be predicted by the BV and DOS-based models as γ and λ are sufficiently small so that $\gamma<10\text{^}(1-\lambda/10k_bT)$. Smaller γ means that the kinetics-governed voltammetric responses extend to potentials further away from $E^{0\prime}$.

To estimate the minimum electrode sizes at which the BV theory can be used to predict the voltammetric responses, Liu et al[34] compared the steady-state polarization curves calculated using different models for ET reactions with various combinations of k^0 and λ at variously sized electrodes. It was shown that for ET reactions with k^0 of around 0.1 cm/s, the BV formalism predicts voltammetric responses visibly deviate from that expected by Eqn (14) as the electrode radius is smaller than 50 nm, while this occurs as r_0 approaches 10 nm for ET reactions with ca. 1.0 cm/s k^0. According to the half-wave-potential difference in the predicted polarization curves, the deviation magnitudes in rate constants by the BV-based voltammetric analysis were estimated.

Compton and coworkers[35] have studied ETs at single nanoparticles using numerical simulations and observed non-BV ET-kinetics at relatively larger particles for reactions with small k^0 ($<10^{-3}$ cm/s). They have also conducted systematic simulation and experiment studies on ETs of a range of organic redox molecules at high-speed micro/nanochannel electrodes for comparative evaluation of the BV and DOS-based kinetic models.[36] The numerical simulations using both kinetic models yielded nearly indistinguishable fits of experimental voltammetry for the relatively facile ETs, for example, the one-electron oxidation of 9,10-diphenylanthracene (k^0~1.0 cm/s); whereas for a very sluggish ET, namely, the one-electron reduction of 2-nitropropane ($k^0<10^{-3}$ cm/s), noticeable differences were found in the fits by the two kinetic models. These studies also raise arguments on the importance of non-symmetrised reorganization of the reduction and oxidation processes.[23] The application of the DOS-based formalism in heterogeneous ET kinetics in SECM with nanoscale tip-substrate gap has also been addressed recently.[37,41] The simulated voltammograms were generalized into analytical equations to allow for reliable determination of k^0 and λ, which were applied to treat the experimental results for rapid ET

reactions of ferrocenemethanol and tetracyanoquinodimethane at Pt substrate electrodes[41].

The possibility of using the mathematically more straightforward MH formalism as an alternative to the unfriendly integrals in Eqn (14) has also been explored.[19,34] The two models were found to predict very similar voltammetric responses before the occurrence of the Marcus inversion for ET reaction with λ above 100 KJ/mol (which are typical reorganization energies for simple outer-sphere redox probes) at electrodes as small as a few nanometer in diameters. Only for reaction with relatively small λ (<50 KJ/mol) at electrodes smaller than 5 nm in diameter, visible deviation of MH predication from that of Eqn (14) can be seen. Similar conclusions should also apply for nanogap electrodes systems. Experimental validation of these prediction requires reliable fabrication and characterization of electrodes smaller than 5 nm in sizes and/or gaps, which remain a great challenge of current state.

3.2 Dynamic diffuse EDL effect

The diffuse EDL effect on heterogeneous ET kinetics has been long known since the pioneer treatment by Frumkin in 1933.[1] It is therefore also called Frumkin EDL correction, which modifies the normal BV equation by replacing E with E-φ_1 and by expressing c^{OHP} with the Boltzmann distribution law. This classic correction have been extensively sued in treating the ET kinetics of highly charged redox species.[1] Nazmutdinov et al recently incorporated it into a theoretical model to study the ET at nanowire electrodes.[42] The use of Poisson-Boltzmann theory to determine φ_1 and c^{OHP} in this correction actually have assumed an equilibrium EDL despite the occurrence of ET at interface. When significant mass transport effect is involved in the ET process, the Boltzmann expression of c^{OHP} was given as $c_j^s\exp(-z_jRT\varphi_1/F)$, where c_j^s refers to the concentration of species j at the inner boundary of the CDL.[1] Such a treatment has been based on the ideas that the EDL and CDL are separable and that the EDL structure is independent on ET rate. This may approximately hold at large electrodes at which the EDL is negligible in thickness as compared with the CDL, but would become inappropriate in the case of significant penetration of diffuse EDL into CDL, as in the nanosize and nanogap electrode systems.

To rationally treat the EDL effect at nanoscopic electrochemical interfaces, a dynamic diffuse EDL model has been introduced by He et al.[17] The core idea is that the nanoscopic electrochemical interface as a whole should be considered a dynamic EDL in the course of an ET reaction. It emphasizes not only the effect of diffuse EDL on the concentration distribution of electroactive species as considered in the classic Frumkin correction, but also the alteration of EDL structure due to the high mass transport rate of electroactive ions. This dynamic EDL can be modelled with two closely coupled equations describing respectively the interfacial structure (relation between the electrostatic potential and concentration distributions) and the voltammetric behaviour (current density-potential dependence), which are given in Eqn (15) and (16) respectively for spherical electrodes. The current density i^* (given in a dimensionless form through normalization with the limiting diffusion current density) is involved in Eqn (15). It is therefore called dynamic Poisson-Boltzmann equation. In the meantime, Eqn (16) contains the electrostatic potential distribution terms, Ω_j, which are integral functions of $\exp(-z_jF\varphi/RT)$ for species j (see Ref. 17 for details). In conventional electrochemistry, the EDL structure and the heterogeneous ET kinetics are mostly treated with independent equations. One can find that Eqn (15) could be approximated to the equilibrium Poisson-Boltzmann equation at low current density, while Eqn (16) would reduce to the mass transfer corrected BV equation in classic voltammetric theory as $\exp(-z_jRT\varphi/F)=1$, that is, the electrostatic potentials in CDL are close to zero. These conditions are approximately satisfied in large electrode systems.

$$\nabla^2\varphi = -\frac{1}{\varepsilon\varepsilon_0}\left(\sum c_j^{\,0} e^{-\frac{Z_jF}{RT}\varphi} - i^*\sum c_O^{\,0} z_j\Omega_j e^{\frac{Z_jF}{RT}\varphi}\right) \qquad (15)$$

$$i^* = \left(\gamma^{-1} e^{\frac{\alpha F(E-E^0)}{RT}} e^{(z-\alpha)\frac{F\varphi_1}{RT}} + \Omega_O + \Omega_R e^{\frac{F(E-E^0)}{RT}}\right)^{-1} \qquad (16)$$

Another important issue concerning the dynamic EDL effects on the heterogeneous ET kinetics in nanoscopic electrode systems is the distinct role of the solvent dielectric screening in EDL. As pointed earlier by Bockris,[43] the high electric field strength ($\bar{E}$) would cause significant decrease in the dielectric constant of solvent (ε) in EDL due to dipole orientation, which in turn enhances $\bar{E}$ in EDL due to reduced dielectric screening effect. This coupling between the electrostatic potential and solvent dielectric distributions in EDL, which is generally neglected in conventional voltammetric treatment, has been found to crucially impact the heterogeneous ET kinetics at nanosized electrodes through affecting the EDL structure, as seen in Eqn (15).[17,19]

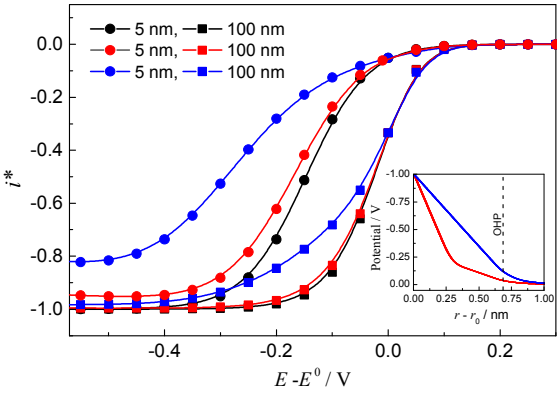

Fig. 4 Steady-state voltammetric responses of spherical electrodes of 5 and 100 nm radii for ET reaction of $O^-+e\rightarrow R^{2-}$ in the presence of excess of supporting electrolyte, predicted by the dynamic EDL model with (red) and without (blue) consideration of ε distribution at interface and by the conventional voltammetric theory considering no EDL effect (black). Inset: Potential distribution in EDL at the 100 nm electrode obtained with (red) and without (blue) consideration of ε distribution.

Considering the short range interaction of water dipoles with electrode as well as the high $\bar{E}$ near electrode surface, it is believed that the first layer of water dipoles are highly oriented (Fig. 1) and form a *saturated dielectric* with ε<=6.[43] Outside the IHP, the value of ε increases gradually with distance due to the decreased $\bar{E}$ and it reaches 78 when $\bar{E}$ becomes very low. The change of ε with $\bar{E}$ can be treated with the Booth equation[40] or simply the average between 6 and 78.[17,19,43] The ignorance of

the ε distribution at interface would overstate the dielectric screening of electric field in EDL, leading to lagged potential distribution in the inner EDL and increased diffuse EDL potentials (the inset of Fig. 4). In result, the EDL effect on the ET kinetics would be overestimated, as indicated by the pronounced deviation of the calculated steady-state voltammetric responses (blue curves in Fig. 4) from that predicted by the conventional voltammetric theory (black curves) even at electrode of 100 nm radius, at which the EDL is expected to be negligible because that the CDL is orders of magnitude thicker than the diffuse EDL. The overestimation of EDL effect on ET kinetics at nanosize electrodes without consideration of dielectric distribution in EDL was also seen in works by others.[18,21] By including the dielectric distribution, the dynamic EDL model predicted voltammetric response nearly identical to that given by the conventional theory at 100 nm electrode, but with visible EDL effect at electrodes a few nanometers in radii (red curves in Fig. 4). It is worth mentioning that the EDL effect on ET kinetics also becomes more pronounced for reactant with higher charge, as well as at smaller electrodes.[17,19]

4. Heterogeneous ETs at sp2 nanocarbons

Carbons in various forms are among the mostly used electrode materials in electrochemistry, both in fundamental studies and technological applications. As the latest members in carbon family, CNTs and graphenes are among the recent electrochemical foci.[44-47] Their intrinsically high specific surface areas and electric conductance offer great promise in constructing high performance electrodes for electrochemical energy and sensing applications. Besides, the distinct electronic structures of these sp^2 nanocarbons make them informative model electrode materials to study electrochemical property-structure relations.

Investigation of structure-dependent electrochemistry of sp^2 carbons can be traced back to the earlier studies of heterogeneous ET kinetics on highly ordered pyrolytic graphite (HOPG), which shares the same basic sp2 carbon structural motif with graphenes and CNTs and represents the most ordered single crystal graphite. As typical semi-metals, graphite materials mostly have rather low DOS near their Fermi levels.[44] For example, theoretical calculation has suggested a ρ_f value of ca. 0.0022 $atom^{-1}$ eV^{-1} for defect-free HOPG basal surface, which is less than 1% of that of Au. This, according to the discussions in Section 2.3, would result in non-adiabatic behavior in heterogeneous ET kinetics, which have been used to interpret the considerably slower heterogeneous ET kinetics observed by some researchers on basal HOPG surfaces than that on the edge planes of graphite.

In the early 1990s, McCreery et al[44,48] reported k^0 values for a range of redox systems on low-defect HOPG surface which are orders of magnitude slower than those on glassy carbons. They believed that it was the many exposed graphitic edges on glass carbon that promote the ET activity, because that the step edges can significantly increase the local DOS. Compton and coworkers[49,50,51] even have concluded that the basal HOPG plane is electrochemically inert and therefore the overall voltammetric responses of an HOPG surface are predominantly contributed by the edge plane sites on it. However, the voltammetric responses obtained with considerably defective HOPG by these authors seemed not showing relatively fast ET kinetics as expected.

The close relationship with graphenes and CNTs has led to a resurgence of interest in the intrinsic electrochemical properties of HOPG during the past a few years. Especially, the traditional consensus that the basal plane has very low or even no electrochemical activity, with step edges contributing nearly all of the voltammetric responses of HOPG surfaces, has been challenged by recent microscopic/nanoscopic studies using various electrochemical scanning microscopies,[52-54] which suggested that the pristine basal surface of HOPG has considerable ET activity. It has been argued that the macroscopic cyclic voltammetry measurements (typically on areas >0.1 cm^2) used in most of the previous studies might not be able to provide reliable kinetics of heterogeneous ET reactions.[52,53] In addition, the possible time-dependent surface passivation effect of ferro/ferricyanide couple, which was used in most of the previous studies, might also have complicated the kinetics determination.[52] To this end, the voltammetric responses of the pristine, freshly cleaved HOPG surface should manifest the electrochemical properties of the basal plane. Although the step edges might be more active, they are such minor sites with densities of only a few percent.[55]

As compared with HOPG, the pristine graphenes and CNTs have even lower (nearly zero) DOS near the Fermi levels, which, however, can be increased greatly in the presence of structural defects and disorders, due to the mid-gap or defect states,[44-47,56] similar to that in silicon. The large DOS increase near Fermi level due to structural disorder in sp2 nanocarbons is manifested in Fig. 5 by taking graphenes for examples.[56] As well as much lower DOS near their Fermi level, these sp^2 nanocarbons have additional structural factors which modulate the electronic structures, e.g., number of layers, sizes and chirality, and layer stacking modes. Thus, one can imagine that graphenes and CNTs would exhibit much more pronounced structure-dependence of heterogeneous ET activity.

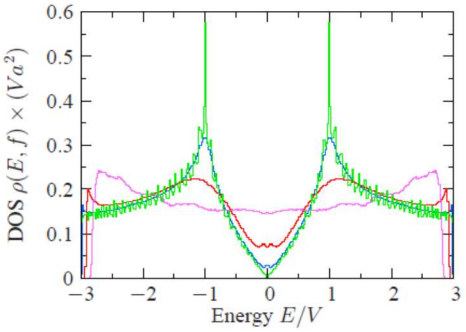

Fig. 5 Calculated DOS distribution for pristine graphene (green curve) and with increasing disorder (black, red, lavender) Reprinted with permission from Ref. 56. Copyright 2009 American Physical Society.

4.1 Importance of structural defects and disorders in the heterogeneous ET kinetics at various graphenes

Graphenes mostly are heterogeneous on their surface, containing bi-/multi-layer islands of different sizes, vacancies, grain boundaries and other structural disorders. The size and fraction of structural defects and disorders depend on the preparation conditions.[45] There are three major types of graphenes: the mechanically exfoliated (ME) graphenes, the chemical vapor deposited (CVD) graphenes, and the reduced graphene oxides (r-GOs). Due to that CVD graphenes can be relatively easily prepared in large-area sheets, they have been the mostly used ones in heterogeneous ET studies.[45]

Abruña and coworkers pioneered the heterogeneous ET study on CVD graphenes. Their recent study using a catalog of redox probes in both aqueous and non-aqueous media showed unexpected quasi-reversible and even nearly reversible ET kinetics,[57] which, together with the unusual values estimated for α, made the authors believe that the ET behaviors on CVD graphenes are likely a composite of factors in addition to basal sp^2 carbon sheets, e.g., defects and/or some adventitious impurities. In an earlier study,[58] they found that the ET kinetics of $Fe(CN)_6^{3-/4-}$ couple was approximately 1 order of magnitude more facile at defects deliberately introduced on CVD graphenes by mechanical damage and/or chemical oxidation than that on the more pristine surfaces. They also showed that the ET kinetics decreased upon passivating the defects. By using SECCM in tandem with Raman microscopy, optical microscopy, and AFM, Unwin and coworkers[59] were able to distinguish the ET activity of the basal domains with that of the multi-layer islands on CVD graphenes. They showed that the heterogeneous ET rates increased systematically with the number of layers, and that the layer stacking also had a subtle influence on ET kinetics. Recent careful investigation exploiting a microinjection-micromanipulator system by Dryfe et al.[60] on the basal surface of differently layered ME graphenes and on the edges/steps between layers also showed an increase in $k°$ with increasing the numbers of graphene layers as well as faster ET kinetics on the edges/steps.

Among various types of graphene materials, r-GOs are the easiest ones for large scale production and application in various electrochemical technologies. Electrochemical studies of r-GOs generally use electrodes of relatively thick films casted on conducting substrates, which makes the measurements of intrinsic electrochemical properties of r-GOs difficult due to the involvement of diversely sized and shaped sheets which have greatly varied defect density, as well as uncontrolled film porosity. Recently, Zhang et al[61] have introduced a nanoelectrode approach to investigate the heterogeneous ET kinetics at individual r-GO flakes. Fig. 6 illustrates the electrode fabrication procedure. Using Au electrodes of submicrometer sizes modified with a self-organized-monolayer (SAM) of n-dodecanethiol, a single mono/few-layer r-GO flake of submicrometer or nanometer size can be attached by quick dipping in dilute r-GO suspensions of corresponding sizes prepared by a size fractionation process. It has been known that the SAM layer can block the ET of Au substrate with redox molecules in solution due to the long distance effect, but allows efficient electron tunneling between Au and the immobilized conducting nanomaterials[62], e.g., r-GO flakes here. Thus, the voltammetric responses of an Au-SAM-r-GO electrode would be dictated by the electrochemical processes at interface between the immobilized single r-GO flake and electrolyte solution. In the meantime, their submicro/nanometer sizes allow measuring the fast heterogeneous ET kinetics with little mass transportation limitation.

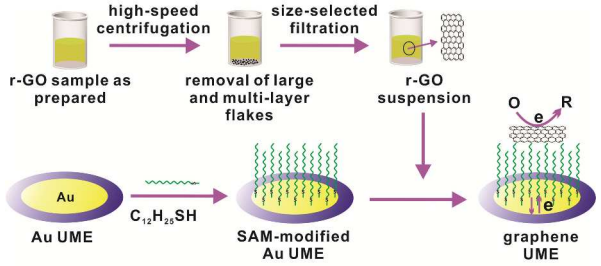

Fig. 6 Schematic illustration of r-GO nanoelectrode fabrication. Reprinted with permission from Ref. 61, copyright 2013, American Chemical Society.

Using r-GO nanoelectrodes described above, Zhang et al[61] obtained k^0 values for the reduction of $Ru(NH_3)_6^{3+}$ and $Fe(CN)_6^{3-}$ on r-GO flakes of a range of sizes, which were much higher than those reported for the same redox probes on HOPGs and the CVD and ME graphenes. Raman measurements on these r-GO flakes exhibited comparable intensity for D and G bands, indicating their defect-dominant nature. More interestingly, the Raman D/G intensity ratios, i.e., the ratios of defects over pristine sp^2 domains, were found to be generally higher for r-GOs of nanometer sizes than those of submicrometer sizes, in accordance with the higher k^0 values obtained on smaller r-GO flakes (Fig. 7). The latter should have undergone more severe oxidation, therefore possess higher fraction of vacancies and edges.

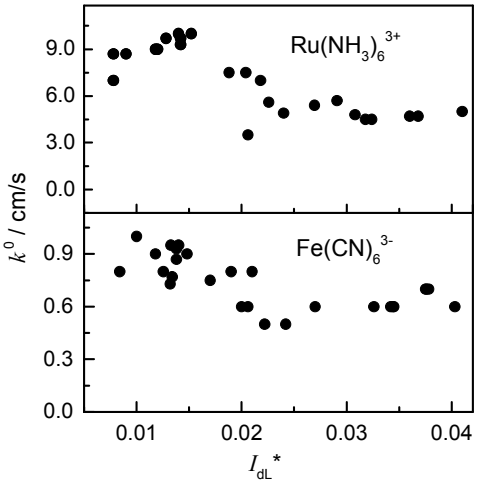

Fig 7. k^0 values obtained for $Ru(NH_3)_6^{3+}$ and $Fe(CN)_6^{3-}$ as functions of r-GO flake sizes represented by the dimensionless limiting currents normalized by the that of a bare Au disk electrode of 5 μm radius. Reprinted with permission from Ref. 61, copyright 2013, American Chemical Society.

4.2 Electronic structure dependent heterogeneous ET activity of single-walled carbon nanotubes

Inspired by the results obtained on HOPGs, considerable research attention on electrochemistry of CNTs has been paid on comparing the heterogeneous ET activity between the sidewalls (pristine sp2 basal surface) and the open ends which are dominated with edge-plane sites. Similarly, a large body of earlier voltammetric studies, which mostly employed electrodes of CNT ensembles drop casted on conducting substrates, have suggested that the pristine CNT sidewalls are poorly active.[46, 63,64] However, recent studies using electrodes of 2D networks of [65] or individual CNTs[66-68] on inert substrates have shown that CNT sidewalls exhibit rather facile ET kinetics for several redox couples. By using their SECCM technique, which combines very high accessible mass-transport rates and the ability of nanoscale mapping of electrochemical activity, Unwin and co-workers very recently have demonstrated nearly uniform ET activity for outer-sphere redox couples across the sidewalls of single-walled CNTs (SWCNTs),[65,68] with SWCNTs of metallic character being as active as metal electrodes. Thus, it seems that the defects and/or edge planes at open ends don't significantly alter the heterogeneous ET activity of CNTs.

As a result of seamless wrapping of graphene sheet into a cylinder along different roll-up vectors, the electronic structures of SWCNTs can be largely modulated by the rolling indices (helicity) which define their diameters and chirality. Depending on the diameters and chirality, SWCNTs can behavior as metal or semiconductors of different band gaps.[46,47] Thus, one would expect that the ET activity of SWCNTs depends on their chirality and sizes. This has been the subject of CNT chemistry since their very first days. The chirality and size dependent charge transfer properties are of particular significance in the functionalization, doping, isolation and purification of CNTs, and their application in molecule sensing, solar cells and redox catalysis.[69-71]

The helicity dependent heterogeneous ET activity of SWCNTs with molecules has been demonstrated in numerous spectro-electrochemical studies. It has been believed that the chiral selectivity in pH-dependent absorbance, Raman and fluorescence spectra of SWCNTs originates in chirality (band gap)-dependent ET reactions.[69] In an earlier study, O'Connell et al[70] investigated the ET reactions between HiPco nanotubes and a range of organic electron-acceptor molecules in solution by redox-induced spectral bleaching. They found obvious diameter and chirality effects on ET kinetics, with rates being the slowest for CNTs with large band gap and increasing for smaller band gap ones. In a recent systematic study by Oelsner et al[71], the ET behavior between semiconducting SWCNTs and the covalently attached electron-donating ferrocene units was shown to be obviously correlated the helicity of SWCNTs. The ET active SWCNTs mostly have large chirality angles, while those having relatively small chirality angles were found to lack ET activity. The authors also showed that only the intermediately sized nanotubes (i.e., 0.92-1.1 nm) were susceptible to accept electrons from ferrocene, while the smaller (i.e., 0.78-0.87 nm) and larger sized nanotubes (i.e., 1.11-1.2 nm) were obviously inert toward charge transfer. The helicity dependent ET activity of SWCNTs has also been revealed by the recent studies on the charge transfer between SWCNTs of distinct chiral vectors and fullerenes of various molecular weights,[72,73] which is of particular significance in emerging photovoltaic and optoelectronic application of CNTs.

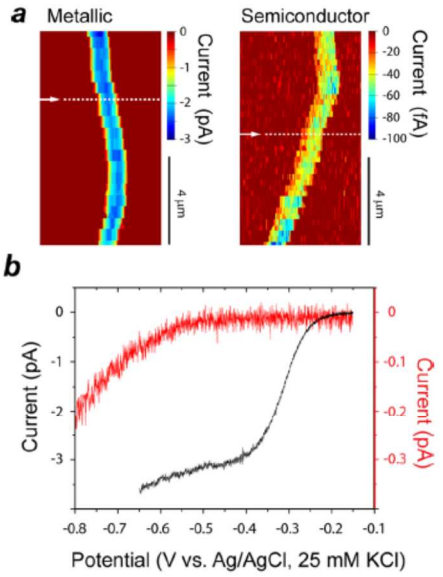

Fig. 8 (a) Voltammetric current maps (at -0.35 V for metallic and -0.65 V for semiconductor SWCNTs) and (b) linear sweep voltammograms (black line for metallic, left-hand y-axis; red line for semiconductor SWNT, right-hand y-xis) at 50 mV s^{-1} obtained using SECCM setup for the reduction of 0.5 mM $Ru(NH_3)_6^{3+}$ (25 mM KCl and phosphate buffer, pH = 7.2) at SWCNT devices. Reprinted with permission from Ref. 68, copyright 2014, American Chemical Society.

Direct electrochemical comparison of heterogeneous ET activity of metallic and semiconductor SWCNTs has been conducted in the recent SECCM study by Unwin and co-workers[68] for two widely studied outer-sphere redox reactions: the oxidation of ferrocenylmethyl-trimethylammonium ($FcTMA^+$) and the reduction of $Ru(NH_3)_6^{3+}$. As well as the high mass transport rate and high spatial resolution, the very low currents inherent to the SECCM make it almost immune to the ohmic drop effect associated with the large Schottky barrier for electron injection in metal-semiconductor contact in CNT electrode device, thus allowing relatively reliable determination of fast ET kinetics on individual SWCNTs. For the oxidation of $FcTMA^+$, the SECCM responses revealed very facile ET kinetics at both the metallic and semiconducting SWCNT devices, with k^0 = 7 ± 2 cm s^{-1} and 4 ± 2 cm s^{-1} respectively. Such a relatively small difference in ET kinetics for $FcTMA^+$ at the two types of SWCNTs was believed to be due to that in the potential range of $FcTMA^+$ oxidation the p-type semiconductor SWCNT is in the charge accumulation state and is therefore metal-like. For the reduction of $Ru(NH_3)_6^{3+}$, whose redox potential lies in the charge depletion region of semiconductor SWCNTs, the two types of SWCNTs exhibit much different ET activity, as indicated by the obtained voltammetric current maps (Fig. 8a) and linear sweep voltammograms recorded with a static SECCM probe centered over the SWCNTs (Fig. 8b). The metallic SWCNT exhibits high and uniform activity, yielding a k^0 of 10 ± 5 cm s^{-1}, which is comparable to that obtained on metal nanoelectrodes. On the semiconductor SWCNT, voltammetric currents were only measurable at high

driving potentials, indicating much inferior ET activity of the semiconductor SWCNTs.

5. Heterogeneous ET at semiconductor nanoparticles

Semiconductor nanoparticles (also called quantum dots, QDs), owing to their unique optoelectronic properties, can be a promising alternative to organic molecular dyes in a variety of applications spanning analytical sciences, diagnostics, and energy conversion. Modern material chemistry allows precise control of size, morphology and composition in nanoparticle synthesis, making their electronic structures flexibly tunable. Especially, semiconductor QDs also possess depleted DOS near their Fermi level, therefore should exhibit dependence of ET kinetics on sizes, shapes and compositions.

Nanoparticle ET processes can be investigated by using either electrochemical or spectroscopic methods. For electrochemical voltammetric measurements, a direct way is to cast them into thin films on conducting substrate. In this case, the voltammetric responses of the resulted electrodes may not reflect the behavior of physically isolated particles as a consequence of the aggregation of nanocrystals. Nanoparticle ET behaviors can also been voltammetrically studied by attaching them to substrate electrodes by using SAMs of organic molecules as linkers. This method is also used in heterogeneous ET studies of other nanomaterials, for example, r-GO sheets, as described in Section 4. Such metal-SAM-nanomaterials hybrid electrodes have applications in electrochemical sensors, photovoltaics and optoelectronics.[62,74]

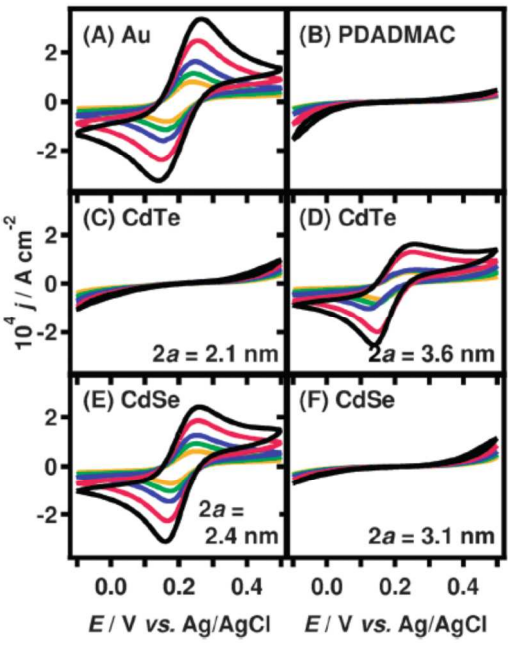

Fig 9. Cyclic voltammograms involving $Fe(CN)6^{3-/4-}$ at a bare Au electrode (A), after modification by mercaptoundecanoic acid (MUA) and poly(diallyldimethylammonium chloride) (PDAMAC) (B) and after adsorption of 2.1 (C) and 3.6 nm (D) CdTe dots, as well as 2.4 (E) and 3.1 nm (F) CdSe dots. Reprinted with permission from Ref. 74, copyright 2011, Royal Chemical Society.

Using the SAM-attaching method, Fermín et al recently investigated the ET behaviors of differently sized CdTe and CdSe QDs with $Fe(CN)_6^{3-/4-}$ redox couple dissolved in solution.[74,75] Fig. 9 shows some example results. Au loses its ET activity nearly completely upon modification of molecular layers (Fig. 9A-B). When CdTe nanoparticles of respectively 2.1 nm and 3.6 nm were attached on the end surface of the modified molecular layers, completely different responses were observed. The 2.1 nm particles exhibited little ET activity (Fig. 9C), while well-defined voltammetric peaks were developed in the presence of 3.6 nm QDs (Fig. 9D). The authors rationalized the electrochemical contrast between the two differently sized CdTe dots in terms of the size-dependent valence band edge level (ε_{VB}).[75] The difference between ε_{VB} and the redox Fermi energy (E^0) of $Fe(CN)_6^{3-/4-}$ determines the DOS overlap area between the QDs and redox molecules (Fig. 3). Actually, the authors also observed partial electrochemical rectification for some middle particle sizes as ε_{VB} approaches E^0. The gap from ε_{VB} to the E^0 of $Fe(CN)_6^{3-/4-}$ was estimated to decrease from ca. 340 to 6 meV upon increasing the CdTe diameter from 2.1 to 3.6 nm. The conduction band negligibly contributes to ET since that ε_{CB} is more than 2 eV above E^0. As shown in Fig. 9E-F, the CdSe QDs exhibit a rather different particle size effect in ET activity from CdTe. The ε_{VB} of CdSe dots are located even below that of the 2.1 nm CdTe particles. The significant ET activity of 2.4 nm CdSe particles (Fig. 9E) may be due to the presence of DOS within the band gap.

Numerous recent spectroscopic studies of ET behaviors of QDs with redox molecules and metal oxides (e.g., SnO_2, TiO_2, and ZnO) also have showed strong dependence of ET rates on ε_{VB}~E^0 gaps which vary with the composition and sizes of QDs.[76-78] In addition, the discreteness of electronic levels of QDs near band edges due to the quantum confinement effect makes their ET with oxide nanoparticles exhibit molecule-solid like ET behavior shown in Fig. 3. For instances, it has been shown that the existence of a continuum of conduction band states and the increasing density at higher energy in metal oxides make ET rates between QDs and oxides increase at driving forces even when it far exceeds the reorganization energy of QDs.[77,78]

6. Possible EDL effects related to the quantum capacitance of low DOS nanomaterials

The low DOS at/near Fermi level in nanomaterials such as sp2 nanocarbons and semiconductor QDs not only decreases the overall electronic overlap with redox probes, but could also modify the EDL structures through the so-called quantum capacitance. For low DOS materials, a relatively small amount of electron injection/extraction (charges) could result in large variation of Fermi energy level relative to the bottom of energy band, i.e., large variation of the chemical potential of electron in electrode. Thus, one can imagine that a certain change in electrode potential would result in significantly decreased charge and electrostatic potential at electrodes of low DOS nanomaterials as compared to bulk metal electrodes, as indicated by Eqn (1). This would make the EDL more diffuse due to the decreased electrostatic interaction. Considering the largely varied electronic structures of low DOS nanomaterials

with the sizes, shapes, doping, chirality and structural disorders, it is expected that electrodes of low DOS nanomaterials would exhibit rich EDL effects on heterogeneous ET kinetics, especially when individual CNTs, graphene nanoribbons or quantum dots are used as nanoelectrodes so that the dynamic EDL effects described in Section 3 arise.

The importance of quantum capacitance on the heterogeneous ET kinetics of sp^2 nanocarbons has been recognized and discussed in an earlier theoretical study by Heller et al.[47] The authors qualitatively addressed its effect on the DOS alignment and overlap in voltammetric measurements. They also predicted that the semiconductor or metallic SWCNT band structure and their distinct van Hove singularities can be resolved in voltammetry. However, the possible coupling of the quantum capacitance with the EDL effects was not considered.

In fact, there still lack quantitative theoretical and experimental studies on the electronic structure dependence of heterogeneous ET kinetics at CNTs and graphenes, and other nanomaterials, although extensive studies over the past two decades have shown obvious correlation between the heterogeneous ET kinetics and electronic structures of low DOS nanomaterials. Systematic quantum-based theoretical calculation incorporating the dynamic EDL model, and detailed comparison of theoretical prediction with reliable voltammetric results obtained on nanomaterials electrodes, especially nanoelectrodes of individual CNTs, graphene nanoribbons and/or single quantum dots are expected to provide more quantitative insights in this area. In fact, the fabrication of nanoelectrodes using individual CNTs has been demonstrated.[66]

7. Summary and outlook

We have summarized the recent insights into the electronic and EDL structure effects in the heterogeneous outer-sphere ET processes in nanoscopic electrode systems, first providing fundamental views on how the electronic and EDL structure effects may be boosted by nanosization of electrodes and/or electrode materials, and then highlighting recent examples in representative electrode systems including electrodes of nanometer sizes and nanometer gaps and of low DOS nanomaterials such as graphenes, carbon nanotubes, and semiconductor quantum dots. The nanoscopic electronic and EDL structure effects are shown to arise due to two types of nanoconfinements: electrode interface and electrode materials.

Reducing the electroactive sizes of an electrode or gaps between two biased electrodes into nanometer scales confines the redox processes into nanoscopic interfacial domains, which leads to an EDL nature of the entire interface, and accordingly pronounced EDL effect on heterogeneous ET kinetics. The nanoconfinement of electrode interface also results in greatly increased mass transport rates, which make the EDL structure highly dynamic so that the classic Frumkin treatment of the diffuse EDL effect becomes inappropriate, and the DOS overlap between electrode and redox molecules important in heterogeneous ET kinetics, as well as the linear energy relation assumed in BV theory problematic.

Nanoconfinement in electrode materials such as 0-D quantum dots, 1-D CNTs and 2-D graphenes result in very low DOS near the Fermi level, which makes their electronic structures vitally important in the heterogamous ET behaviors due to the decreased adiabaticity. Since the electronic structures of these nanomaterials are strongly size and morphology dependent, the voltammetric responses as functions of physical structures should help to reveal the relation between the electronic structures and sizes and morphologies of these materials.

We expect that a combination of the interface and material confinements, by using individual CNTs, graphene nanoribbons or quantum dots as nanoelectrodes, would raise rich size and structure effects in heterogeneous ET behaviors. It calls systematic quantum-based theoretical calculation incorporating the dynamic EDL model, aw well as reliable electrode fabrication and characterization studies.

Acknowledgements

The authors thank the financial supports from the Ministry of Science and Technology of China (Grant No. 2012CB932800, 2013AA110201 and 2012CB215500) and National Natural Science Foundation of China (21173162, 21073137 and 20973131).

Notes and references

Hubei Key Laboratory of Electrochemical Power Sources, Key Laboratory of Analytical Chemistry for Biology and Medicine (Ministry of Education), Department of Chemistry, Wuhan University, Wuhan 430072, China. Tel & Fax: 027-68754693; E-mail: slchen@whu.edu.cn.

1 A. J. Bard and L. R. Faulkner, *Electrochemical methods: fundamentals and applications*, 2nd ed., John Wiley & Sons, New York, 2001.
2 R. Marcus, *Annu. Rev. Phys. Chem*., 1964, 15, 155-196.
3 A. J. Bard, *J. Am. Chem. Soc*., 2010, 132, 7559-67.
4 X.-S. Zhou, L. Liu, P. Fortgang, A.-S. Lefevre, A. Serra-Muns, N. Raouafi, C. Amatore, B.-W. Mao, E. Maisonhaute, B. Schöllhorn, *J. Am. Chem. Soc*., 2011, **135**, 7509–7516.
5 J. T. Cox, B. Zhang, *Annu. Rev. Anal. Chem*., 2012, **5**, 253-272.
6 S. M. Oja, M. Wood, B. Zhang, *Anal. Chem.*,2013, **85**, 473.
7 S. J. Liu, Q. Li, Y. H. Shao, *Chem. Soc. Rev*., 2011, **40**, 2236-2253.
8 L. Rassaei, P. S. Singh, S. G. Lemay, *Anal. Chem*., 2011, 83, 3974–3980.
9 X. Cao, N. Wang, S. Jia, and Y. H. Shao, *Anal. Chem.*, 2013, **85**, 5040–5046.
10 Q. F. Zhang, E. Uchaker, S. L. Candelaria, G. Z. Cao, *Chem. Soc. Rev*., 2013, **42**, 3127-3171.
11 H. J. You, S. C. Yang, B. J. Ding, H. Yang, *Chem. Soc. Rev*., 2013, **42**, 2880-2904.
12 N. Sato, *Electrochemistry at Metal and Semiconductor Electrodes*, Elsevier Science, Amsterdam, 1998.
13 J. O'M. Bockris, M. A.V. Devanathan, K. Muller, *Proc. R. Soc. Lond. A*., 1963, **274**, 55-79.
14 J. Velmurugan, P. Sun, M. V. Mirkin, *J. Phys. Chem. C*., 2009, **113**, 459–464.
15 T. Iwasita, W. Schmickler, J. W. Schultze, *Ber. Bensunges. Phys.*

Chem., 1985, **89**, 138
16 T. Iwasita, W. Schmickler, J.W. Schultze, *J. Electroanal. Chem*., 1985, **194**, 355.
17 R. He, F. Yang, S. L. Chen, B. L. Wu, *J. Phys. Chem. B*., 2006, 110, 3262–3270
18 E. J. F. Dickinson, R. G. Compton, *J. Electroanal. Chem.*, 2011, **661**, 198–212.
19 S. L. Chen , Y. W. Liu, *Phys. Chem. Chem. Phys.*, 2014, **16**, 635-652.
20 J. D. Norton, H. S. White , S. W. Feldberg, *J. Phys. Chem.*, 1990, **94**, 6772-6780.
21 C. P. Smith, H. S. White, *Anal. Chem*., 1993, **65**, 3343-3353.
22 N. S. Hush, *J. Chem. Phys*., 1958, **28**, 962 – 972.; *J. Electroanal. Chem.*, 1999, **470**, 170-195.
23 E. Laborda, M. C. Henstridge, C. Batchelor-McAuley, R. G. Compton, *Chem. Soc. Rev*., 2013, **42**, 4894-4905.
24 M.D. Newton, N. Sutin, *Annu. Rev. Phys. Chem.*, 1984, **35**, 437.
25 V. G. Levich, in *Physical Chemistry: An Advanced Treatise Vol. 9B*, ed. H. Eyring, D. Henderson and W. Jost, Academic, New York, 1970.
26 H. Gerischer, *Photochem. Photobiol*., 1972, **16**, 243 – 260.
27 W. Schmickler, *J. Electroanal. Chem.,* 1986, **204**, 31.
28 C. E. D. Chidsey, *Science*., 1991, **251**, 919-922.
29 H. O. Finklea, D. D. Hanshew, *J. Am. Chem. Soc*., 1992, **114**, 3173-3181.
30 A. M. Becka, C. J. Miller, *J. Phys. Chem*., 1992, **96**, 2657-2668.
31 R. R. Dogonadze, A. M. Kuznetsov, M. A. Vorotyntsev, *J. Electroanal. Chem.*, 1970, **25**, A17.
32 S. W. Feldberg, *Anal. Chem*., 2010, **82**, 5176–5183.
33 H. V. Patten, K. E. Meadows, L. A. Hutton, J. G. Iacobini, D. Battistel, K. McKelvey, A. W. Colburn, M. E. Newton, J. V. Macpherson, P. R. Unwin, *Angew. Chem. Int. Ed.*, 2012, **51**, 1.
34 Y. W. Liu, S. L. Chen, *J. Phys. Chem. C*., 2012, **116**, 13594−13602.
35 M. C. Henstridge, K. R. Ward, R. G. Compton, *J. Electroanal. Chem*., 2014, **712**, 14–18.
36 D. Suwatchara , M. C. Henstridge , N. V. Rees , R. G. Compton, *J. Phys. Chem. C*., 2011, **115**, 14876–14882.
37 S. Amemiya, N. Nioradze, P. Santhosh, M. J. Deible, *Anal. Chem*., 2011, **83**, 5928–5935.
38 M. V. Mirkin, Y. X. Wang, J. Velmurugan, *Isr. J. Chem*., 2010, **50**, 291−305.
39 M. A. G. Zevenbergen, B. L. Wolfrum, E. D. Goluch, P. S. Singh, S. G. Lemay, *J. Am. Chem. Soc*., 2009, **131**, 11471–11477.
40 Y. W. Liu, R. He, Q. F. Zhang , S. L. Chen, *J. Phys. Chem. C*., 2010, **114**, 10812 – 10822.
41 M. N. Nioradze , J. Kim, S. Amemiya, *Anal. Chem.*, 2011, **83**, 828–835.
42 R. R. Nazmutdinova, M. D. Bronshteina, W. Schmickler, *Electrochimica. Acta*., 2009, **55**, 68-77.
43 J. O. M. Bockris, A. K. N. Reddy, in Modern Electrochemistry, Plenum: New York, 1970; Vol.2.
44 R. L. McCreery, M. T. McDermott, *Anal. Chem*., 2012, **84**, 2602−2605. And references wherein.
45 D. A. C. Brownson, D. K. Kampouris, C. E. Banks, *Chem. Soc. Rev*., 2012, **41**, 6944–6976.
46 I. Dumitrescu, P. R. Unwin, J. V. Macpherson, *Chem. Commun*., 2009, 6886-6901. And references wherein.
47 I. Heller, J. Kong, K. A. Williams, C. dekker, S. G. Lemay, *J. Am. Chem*. Soc., 2006, **128**, 7353−7359.
48 R. L. McCreery, *Chem. Rev*., 2008, **108**, 2646. And references wherein.
49 T. J. Davies, R. R. Moore, C. E. Banks, R. G. Compton, *J. Electroanal. Chem*., 2004, **574**, 123-152.
50 C. E. Banks, T. J. Davies, G. G. Wildgoose, R. G. Compton, *Chem. Commun*., 2005, 829.
51 C. E. Banks, R. R. Moore, T. J. Davies, R. G. Compton, *Chem. Commun*., 2004, 1804.
52 C. S. S. Lai, A. N. Patel, K. McKelvey, P. R. Unwin, *Angew. Chem., Int. Ed.*, 2012, **51**, 5405.
53 A. N. Patel, M. G. Collignon, M. A. O'Connell, W. O. Y. Hung, K. McKelvey, J. V. Macpherson, P. R. Unwin, *J. Am. Chem. Soc.*, 2012, **134**, 20117. And references wherein.
54 A. Anne, E. Cambril, A. Chovin, C. Demaille, C. Goyer, *ACS Nano* 2009, **3**, 2927.
55 H. Chang, A. J. Bard, *Langmuir*, 1991, **7**, 1143−1153).
56 L. Schweitzer, *Phys. Rev. B*., 2009, **80**, 245430.
57 N. L. Ritzert, J. Rodríguez-López, C. Tan, H. D. Abruña, *Langmuir*., 2013, **29**, 1683–1694.
58 C. Tan, J. Rodríguez-López, J. J. Parks, N. L. Ritzert, D. C. Ralph, H. D. Abruña, *ACS nano*., 2012, **6**, 3070-3079.
59 A. G. Güell, N. Ebejer, M. E. Snowden, J. V. Macpherson, P. R. Unwin, *J. Am. Chem. Soc*., 2012, **134**, 7258-7261.
60 P. S. Toth, A. T. Valota, M. Velický, I. A. Kinloch, K. S. Novoselov, E. W. Hill, R. A. W. Dryfe, *Chem. Sci*., 2014, **5**, 582-589.
61 B. Zhang, L. X. Fan, H. W. Zhong, Y. W. Liu, S. L. Chen, *J. Am. Chem. Soc*., 2013, **135**, 10073–10080.
62 J.-N. Chazalviel, A. Philippe, *J. Am. Chem. Soc*., 2011, **133**, 762–764.
63 C. E. Banks, R. R. Moore, T. J. Davies, R. G. Compton, *Chem Commun*, 2004, 1804.
64 A. Chou, T. Bocking, N. K. Singh, J. J. Gooding, *Chem Commun.*, 2005, 842–844.
65 A. G. Güell, N. Ebejer, M. E. Snowden, K. McKelvey, J. V. Macpherson, P. R. Unwin, *Proc. Natl. Acad. Sci. U.S.A.*, 2012, **109**, 11487−92. And references wherein
66 I. Heller, J. kong, H. A. Heering, K. A. Williams, S. G. Lemay, C. Dekker, *Nano Letters*., 2005, **5**, 137-142.
67 J. Kim, H. Xiong, M. Hofmann, J. Kong, S. Amemiya , *Anal. Chem.*, 2010, **82**, 1605–1607.
68 A. G. Güell, K. E. Meadows, P. V. Dudin, N. Ebejer, J. V. Macpherson, P. R. Unwin, *Nano Lett.*, 2014, **14**, 220–224.
69 M. Zheng, B. A. Diner, *J. Am. Chem. Soc*., 2004, **126**, 15490-15494.
70 M. J. *O'Connell*, E. E. Eibergen, S. K. Doorn, *Nature Materials*., 2005, **4**, 412-418.
71 C. Oelsner, M. A. Herrero, C. Ehli, M. Prato, D. M. Guldi, *J. Am. Chem. Soc*., 2011, **133**, 18696-18706.
72 C. M. Isborn, C. Tang, A. Martini, E. R. Johnson, A. Otero-de-la-Roza, V. C. Tung, *J. Phys. Chem. Lett*., 2013, **4**, 2914–2918.
73 A. J. Hilmer, K. Tvrdy, J. Q. Zhang, M. S. Strano, *J. Am. Chem. Soc*., 2013, **135**, 11901–11910.
74 G. P. Kissling, D. O. Milesa, D. J. Fermín, *Phys. Chem. Chem. Phys.,* 2011, **13**, 21175–21185. And references wherein.
75 G. P. Kissling, C. Bünzli and D. J. Fermín, *J. Am. Chem. Soc.*, 2010, **132**, 16855–16861.

76 J. Huang , Z. Huang , Y. Yang , H. Zhu, T. Q. Lian, *J. Am. Chem. Soc.*, 2010, **132**, 4858–4864
77 K. Tvrdy, P. A. Frantsuzov, P. V. Kamat, *Proc. Natl. Acad. Sci. U.S.A.* 2011, **108**, 29.
78 K. Žídek, K. Zheng, C. S. Ponseca, M. E. Messing, L. R. Wallenberg, P. Chábera, M. Abdellah, V. Sundström, T. Pullerits, *J. Am. Chem. Soc.* **2012**, 134, 12110.

